

A Lower Limit on $\Omega_m - \Omega_\Lambda$ Using the Gravitational Lensing Rate in the Hubble Deep Field

Asantha R. Cooray, Jean M. Quashnock, M. Coleman Miller

Department of Astronomy and Astrophysics, University of Chicago, Chicago IL 60637
E-mail: asante@hyde.uchicago.edu, jmq@oddjob.uchicago.edu, miller@bayes.uchicago.edu

ABSTRACT

We calculate the expected strong gravitational lensing rate in the Hubble Deep Field (HDF) by using photometric redshift information for galaxies present in all four HDF passbands with a I-band magnitude limit of 27. A comparison of these predictions with the observed number of strongly lensed sources places a lower limit on the current value of $\Omega_m - \Omega_\Lambda$, where Ω_m is the cosmological mass density of the universe and Ω_Λ is the normalized cosmological constant. Based on current estimates of the HDF luminosity function and associated uncertainties in individual parameters, our 95% confidence lower limit on $\Omega_m - \Omega_\Lambda$ is between -0.17, if there are no strongly lensed sources in the HDF, and -0.59, if there are three strongly lensed sources in the HDF. For a flat universe ($\Omega_m + \Omega_\Lambda = 1$), $\Omega_\Lambda < 0.58$ to 0.79 (95% C.L.). If the only lensed source in the HDF is the one presently viable candidate, then $\Omega_m - \Omega_\Lambda > -0.39$. These lower limits are compatible with estimates based on high redshift supernovae and with previous limits based on gravitational lensing.

Subject headings: cosmology: observations — galaxies: luminosity function — gravitational lensing

1. INTRODUCTION

The Hubble Deep Field (HDF) is the deepest optical survey that has been performed to date, allowing detailed studies of the galaxy redshift distribution (see, e.g., Gwyn & Hartwick 1996) and the global star formation history (see, e.g., Madau et al. 1996, 1998). The HDF covers an area of 4.3 arcmin^2 , with a pixel scale of $0''.04 \text{ pixel}^{-1}$, and has a point source detection threshold of 27.0, 29.5, 29.5 and 28.5 mag in U-, B-, V-, and I-band data. Complete observational and data reduction details of the HDF are given by Williams et al. (1996).

Spectroscopic redshifts exist for nearly 180 sources in the HDF. These redshifts are now complemented by two photometric redshift catalogs, one based on spectral template fitting (Sawicki, Lin, & Yee 1997; hereafter SLY), and the other on empirical color-redshift relations (Wang, Bahcall, & Turner 1998; hereafter WBT). Galaxies in the HDF have redshifts which are estimated to range

from 0.1 to 5, with a large portion having redshifts between 2 and 4, suggesting that some may be strongly lensed. The Hubble Space Telescope (HST) has proven to be a valuable observatory for gravitational lens discovery programs because of the high resolution images it produces (see, e.g., Ratnatunga et al. 1995). The combination of high resolution and deep exposures in multiple colors was expected to provide a rich ground for gravitational lens searches, and it was expected that HDF would contain somewhere between 3 to 10 lenses based on the lensing rate for quasars and radio sources (see, e.g., Hogg et al. 1996).

Instead, a careful analysis of the HDF (see, e.g., Zepf et al. 1997) has revealed a surprising dearth of candidates for lensed sources. In fact, the best estimate is either 0 or 1 lensed sources in the entire field, although very faint images with small angular separations may have escaped current analyses. This lack of lensing has led to suggestions (see, e.g., Zepf et al. 1997) that the HDF data may be incompatible with the high lensing rate expected in universes dominated by a cosmological constant.

Here, we calculate the expected rate of detected lensing in the HDF for different cosmological parameters, and we constrain these parameters by comparing the predictions with the observations. In § 2 we discuss our calculation and its inputs, including the inferred redshifts of the galaxies and the luminosity distribution of potential lenses. In § 3 we present our resulting constraints on cosmological parameters, and in particular on $\Omega_m - \Omega_\Lambda$. In § 4 we discuss the potential effect of systematic errors in the predicted and observed rate of strong lensing. Finally in § 5 we summarize and discuss future prospects for tighter constraints. We follow the conventions that the Hubble constant, H_0 , is $100 h \text{ km s}^{-1} \text{ Mpc}^{-1}$, the present mean density in the universe in units of the closure density is Ω_m , and the present normalized cosmological constant is Ω_Λ . In a flat universe, $\Omega_m + \Omega_\Lambda = 1$.

2. EXPECTED AND OBSERVED LENSING RATE

In this section we describe our calculation of the expected lensing rate. In § 2.1 we discuss the formalism for the calculation, and in § 2.2 we consider input quantities and their errors, such as the photometric redshifts and the luminosity distribution of potential lenses.

2.1. Expected Lensing Rate in the HDF

In order to calculate the lensing rate for HDF galaxies, we model the lensing galaxies as singular isothermal spheres (SIS) and use the analytical filled-beam approximation (see, e.g., Fukugita et al. 1992). At redshifts $z \lesssim 4$, the analytical filled-beam calculations in Fukugita et al. (1992) agree to better than 2% with numerical calculations (see, e.g., Fig. 1 in Holz, Miller, & Quashnock 1998).

In addition, it is necessary to take into account two further effects. First, any magnitude-

limited sample such as the HDF is subject to so-called “magnification bias” (see, e.g., Kochanek 1991), in which the number of lensed sources in the sample is larger than it would be in an unbiased sample, because lensing brightens sources that would otherwise not be detected into the sample. This is a particularly pronounced effect in quasar lensing surveys (see, e.g., Maoz & Rix 1993), because the faint end of the quasar luminosity function rises steeply. Second, because identification of a lensed source requires the detection of at least two of its multiple images, then if the second brightest of the images is too faint to detect, such sources will not be identified as strongly lensed. For lens-search surveys such as the HST Snapshot Survey of bright quasars (Bahcall et al. 1992), this effect is small, because the depth of the pointed search is much greater than the depth of the initial search, and hence almost all secondary images will be detected. In the case of the HDF, it is not possible to do a deeper follow-up, and hence for a significant fraction of sources, especially near the limiting magnitude of the survey, it will be difficult to detect other lensed companions.

If the probability for a source at redshift z to be strongly lensed is $p(z, \Omega_m, \Omega_\Lambda)$, and the number of unlensed sources in the HDF between rest-frame luminosity L and $L + dL$ and between redshifts z and $z + dz$ is $\Phi(L, z)dL dz$, then the number of lensed sources, $d\bar{N}$, in that luminosity and redshift interval expected in the HDF is (see also Maoz et al. 1992)

$$d\bar{N}(L, z) = p(z, \Omega_m, \Omega_\Lambda) dz \int \left[\Phi \left(\frac{L}{A}, z \right) \frac{dL}{A} \right] f(A, L, z) q(A) dA, \quad (1)$$

where the integral is over all allowed values of A , the amplification of the brightest lensed image compared to the unlensed brightness, $q(A)$ is the probability distribution of amplifications, and $f(A, L, z)$ is the probability of observing the second-brightest image given A , L , and z . Our assumption that the lenses are singular isothermal spheres implies that the minimum amplification is $A_{\min} = 2$ and the probability distribution is $q(A) = 2/(A - 1)^3$. For simplicity, we will assume that $f(A, L, z)$ is a step function (Θ), so that a dimmer image with apparent magnitude brighter than m_{lim} is detected, whereas one dimmer than m_{lim} is not detected. This assumption means that

$$f(A, L, z) = \Theta \left[m_{\text{lim}} - m_i - 2.5 \log_{10} \left(\frac{A}{A - 2} \right) \right], \quad (2)$$

where m_i is the apparent magnitude of the brighter image and $A/(A-2)$ is the ratio of the brightness of the primary image to the brightness of the secondary image in the SIS approximation.

Let us now assume that the brightness distribution of galaxies at any given redshift is described by a Schechter function, in which the comoving density of galaxies at redshift z and with luminosity between L and $L + dL$ is

$$\phi(L, z) dL = \phi^*(z) \left[\frac{L}{L^*(z)} \right]^{\alpha(z)} e^{-L/L^*(z)} dL, \quad (3)$$

where as before both L and L^* are measured in the rest frame of the galaxy. Thus, $\Phi(L, z) = \phi(L, z) dV/dz$, where V is the comoving volume in the solid angle of the HDF. We can then write

the expected number \bar{N} of lensed galaxies in our selected subsample of the HDF as

$$\begin{aligned} \bar{N} &= \sum_i p(z_i, \Omega_m, \Omega_\Lambda) \int_2^\infty A^{-1-\alpha(z_i)} e^{L_i/L^*(z_i)} e^{-L_i/AL^*(z_i)} \\ &\quad \times \Theta \left[m_{\text{lim}} - m_i - 2.5 \log_{10} \left(\frac{A}{A-2} \right) \right] \frac{2}{(A-1)^3} dA \\ &\equiv \sum_i \tau(z_i) . \end{aligned} \tag{4}$$

Here the sum is over each of the galaxies in our sample, where we have chosen only those galaxies in the HDF with I magnitudes brighter than 27. The index i represents each galaxy; hence, z_i , L_i , and m_i are, respectively, the redshift, rest-frame luminosity, and apparent I magnitude of the i th galaxy.

The quantities z_i and m_i can be measured with relatively little error, but the rest-frame luminosities L_i and $L^*(z_i)$ are more complicated to infer because their value depends on uncertain K-corrections. Therefore, we estimate the total average bias by summing the expectation values of $\tau(z_i)$, which are computed by weighting the integral in equation (4) by a normalized distribution of luminosities L_i drawn from the Schechter function at redshift z_i , instead of using inferred rest-frame luminosities that are very uncertain.

2.2. Uncertainties in Inputs

Redshifts of galaxies—We have used two available photometric redshift catalogs for galaxies in the HDF: SLY used spectral fitting techniques to calculate the redshift for all galaxies that appeared in the four HDF passbands with a I-band limiting magnitude of 27. There are 848 such galaxies, 181 of which have spectroscopic redshifts. Recently, WBT computed photometric redshifts for the same sample as SLY, based on empirical relations which were calibrated against spectroscopic redshifts. In Figure 1, we show the redshift distribution of the HDF galaxies according to the SLY (left panel) and WBT (right panel) catalogs, as a function of the I-band magnitude. These distributions are similar to that found by Gwyn & Hartwick (1996), and contain two peaks, with one at $z \sim 0.6$ and the other at $z \sim 2.3$. Compared to the spectroscopic redshifts, the photometric redshifts of SLY have a larger scatter than the redshifts of WBT. However, as is clear from Fig. 1, there is a pronounced lack of photometric redshifts between 1.5 and 2.2 in the WBT catalog; this gap is much less dramatic in the SLY catalog. It is therefore unclear which catalog is more reliable overall. We therefore estimate cosmological constraints based on both catalogs, but we find (see § 3) that the derived constraints are almost the same for either catalog.

Properties of lensing galaxies—The probability of strong lensing depends on the number density and typical mass of lensing galaxies. For singular isothermal spheres, this factor is conveniently represented by the dimensionless parameter

$$F \equiv 16\pi^3 n_0 R_0^3 \left(\frac{\sigma}{c} \right)^4 . \tag{5}$$

Here n_0 is the number density of galaxies, $R_0 \equiv c/H_0$, and σ is the velocity dispersion. The parameter F is independent of the Hubble constant, because the observationally inferred number density is proportional to h^3 . We can estimate F at a given redshift from the galaxy luminosity function at that redshift, if we assume a dependence of the velocity dispersion on the luminosity. A commonly assumed functional form is $L \propto \sigma^\gamma$, so that $\sigma^4 \propto L^{4/\gamma}$. Kochanek (1996) estimates $\gamma = 4.0 \pm 0.5$ and adopts a velocity dispersion for an L^* galaxy in the local universe of $\sigma = 220 \pm 20$ km s $^{-1}$. If the luminosity function at redshift z is given by equation (3), then with the normalization for the velocity dispersion given by Kochanek (1996), we have

$$F = 3.87 \left[\frac{L^*(z)}{L^*(0)} \right]^{\frac{4}{\gamma}} \phi^*(z) \Gamma \left(\alpha + \frac{4}{\gamma} + 1 \right), \quad (6)$$

where Γ is the normal gamma function. We assume that the luminosity at which $\sigma = 220$ km s $^{-1}$, corresponds to a B magnitude of $M_B^* = -20.7$. Henceforth, we will also assume $\gamma = 4$.

To estimate F , we concentrate on the redshifts between 0.5 and 1.0, because foreground lensing galaxies for most of the presently confirmed lensed sources are in this redshift range (see, e.g., Kochanek 1996). SLY find that in this redshift range, the HDF luminosity function for galaxies is represented by a Schechter function with parameters

$$M_B^* = -19.9 \pm 0.3, \quad \alpha = -1.3 \pm 0.1, \quad \phi^* = 0.042 \pm 0.13 \text{ h}^3 \text{Mpc}^{-3}. \quad (7)$$

The best estimate for F is therefore 0.101. If the errors in the parameters were independent of each other, the uncertainty in F would be at least a factor of 2. However, the parameters in Schechter luminosity function are correlated. For example, in the Century Survey (Geller et al. 1997) the joint error ellipses for α and M^* show that, in the R band, $\alpha \approx -1.2 + (M_R^* + 20.7)$. It is therefore plausible that a similar relation holds for the HDF luminosity function parameters. From Table 1 of SLY, we find that, for z between 0.5 and 1.0, $\alpha \approx -1.3 + 0.3(M_B^* + 19.9)$. In addition, the absolute normalization is well-determined at the faint end of the luminosity function, where there are many galaxies. If we fix the number density at $0.01L^*$, where the galaxies are numerous yet still bright enough to be detected reliably, then a variation in α determines the values of M_B^* and ϕ^* . The 1σ range in α then gives values of F in a tight range, between 0.100 and 0.108. However, the correlation between α and M_B^* is inexact; furthermore, other uncertainties, such as in the velocity dispersion σ , must also be considered. To be conservative, we allow for an overall uncertainty of 30%, and take $F = 0.10 \pm 0.03$.

3. CONSTRAINTS ON COSMOLOGICAL PARAMETERS

3.1. Observed lensing rate in the HDF

The first potential detection of a gravitationally lensed source in the HDF is described in Hogg et al. (1996). However, the candidacy of this object was later questioned by Zepf et al. (1997), who made Keck spectroscopic observations of 3 lens-like objects in the HDF. These three sources were selected based on the morphological distribution of nearly 750 galaxies, down to a limiting magnitude of 27 in the I-band. Discrepancies in the inferred redshifts of the multiple images suggested that two of the three candidates are not lensed sources, leaving one possible gravitational lens in the HDF down to I of 27 (L3.2 in Zepf et al. 1997). It is possible that even this source is not strongly lensed, but currently the data are inconclusive. Zepf et al. (1997) argue that it is unlikely that there is a large population of lensed sources in the HDF that has been missed. This is especially true for sources brighter than $m_I = 27, 1.5$ mag above the detection threshold, m_{lim} , of 28.5 in the I-band. However, in order to take into account the possibility that multiply-imaged sources with faint secondary images (which still have $m_I < 28.5$) or small angular separations have been missed, we calculate cosmological limits based on the assumed detection of 0, 1, 2, or 3 lensed sources with secondary images brighter than $m_{\text{lim}} = 28.5$, $m_{\text{lim}} = 28.0$, and $m_{\text{lim}} = 27.5$ in the HDF. As we discuss in more detail in the next section, the limits that follow from the detection of at least one lensed source require knowledge of the redshift of the background lensed source. The single candidate of Zepf et al. (1997) has an uncertain redshift, but the redshift is most probably in the range $1.0 \lesssim z \lesssim 2.5$, with a best guess of 1.02.

3.2. Comparison of Predicted with Observed Lensing Rate

We have calculated the expected number, \bar{N} , of gravitationally lensed sources in the HDF by using equation (4) for various combinations of Ω_m , Ω_Λ , m_{lim} , and α , the luminosity function power-law slope for galaxies with redshifts between 2 and 3 (the redshift range expected to produce most of the lensed sources in the HDF). We perform each calculation using both the SLY and WBT catalogs. Figure 2 shows the expected number of gravitational lenses in the HDF as a function of Ω_m and Ω_Λ , assuming $m_{\text{lim}} = 28.5$ and $\alpha = -2.1$, and using the SLY photometric redshifts. A universe dominated with Ω_Λ has a higher number of multiply-imaged sources than in a universe dominated with a large Ω_m . As shown in Fig. 2, \bar{N} is essentially a function of the combined quantity $\Omega_m - \Omega_\Lambda$. This degeneracy in the lensing rate (Carroll, Press, & Turner 1992; Kochanek 1993; Holz, Miller, & Quashnock 1998) allows us (see below) to constrain $\Omega_m - \Omega_\Lambda$ rather than Ω_m or Ω_Λ individually. In Table 1, we list the expected number of strongly lensed sources in the HDF along the $\Omega_m + \Omega_\Lambda = 1$ line as a function of $\Omega_m - \Omega_\Lambda$. These expected numbers, which are listed for the two catalogs separately, have been calculated assuming $m_{\text{lim}} = 28.5$ and $\alpha = -2.1$.

3.3. Likelihood Constraints on $\Omega_m - \Omega_\Lambda$

We constrain the quantity $\Omega_m - \Omega_\Lambda$ by comparing the observed and predicted number of lensed sources in the HDF. We adopt a Bayesian approach, and take a prior for $\Omega_m - \Omega_\Lambda$ that is uniform between -1 and +1. We do this because we do not yet have a precise determination of this quantity (although recent high redshift supernovae measurements favor a value near -0.5; see, e.g., Riess et al. 1998), and we do not wish to consider cosmologies in which either Ω_m or Ω_Λ lie outside the interval [0,1]. We do not constrain Ω_m or Ω_Λ separately; thus, no prior is required for these quantities. Since the prior for $\Omega_m - \Omega_\Lambda$ is uniform, the posterior probability density is simply proportional to the likelihood (see below).

From equation (4), $\bar{N} = \sum_i \tau(z_i)$, where $\tau(z_i)$ is the effective probability that a source at redshift z_i is lensed. Here, $\tau(z_i)$ and \bar{N} depend on $\Omega_m - \Omega_\Lambda$, and are directly proportional to the dimensionless parameter F defined in equation (5). Furthermore, we take into account the uncertainty in F by defining $\mathcal{F} \equiv F/0.1$ and taking \mathcal{F} to have a mean of unity and standard deviation $\sigma_{\mathcal{F}} = 0.3$. Thus, we allow for a 30% uncertainty in F (see § 2). The factor \mathcal{F} is then an overall correction to the expected lensing rate, due to a systematic uncertainty in F .

The likelihood \mathcal{L} — a function of $\Omega_m - \Omega_\Lambda$ — is the probability of the data, given $\Omega_m - \Omega_\Lambda$. If there are no lensed sources in the HDF, and if \mathcal{F} were known exactly, this probability would be

$$\begin{aligned} \mathcal{L}(0) &= \prod_i e^{-\mathcal{F}\tau(z_i)} = e^{-\mathcal{F}\bar{N}} \\ &= e^{-\bar{N}} \times e^{-(\mathcal{F}-1)\bar{N}} . \end{aligned} \quad (8)$$

We account for the uncertainty in F by marginalizing the above expression over $\mathcal{F} = 1.0 \pm \sigma_{\mathcal{F}}$, expanding the exponential, and taking expectation values. To second order in $\sigma_{\mathcal{F}}$, we find

$$\langle \mathcal{L}(0) \rangle = e^{-\bar{N}} \times \left(1 + \sigma_{\mathcal{F}}^2 \frac{\bar{N}^2}{2} \right) . \quad (9)$$

We only include contributions from the variance in \mathcal{F} to the expectation value, since we do not know the exact distribution (and higher moments) of \mathcal{F} . In any case, the contribution of higher-order terms to our lower limits on $\Omega_m - \Omega_\Lambda$ are negligible.

If instead, there is one lensed source (at redshift z_j) in the HDF, and if \mathcal{F} were known exactly, the likelihood would be

$$\begin{aligned} \mathcal{L}(1) &= \mathcal{F}\tau(z_j) \times \prod_i e^{-\mathcal{F}\tau(z_i)} = \tau(z_j) \times \mathcal{F}e^{-\mathcal{F}\bar{N}} \\ &= \tau(z_j) \times \left(-\frac{\partial \mathcal{L}(0)}{\partial \bar{N}} \right) . \end{aligned} \quad (10)$$

By again marginalizing over \mathcal{F} , and substituting equation (9) into equation (10), we obtain

$$\langle \mathcal{L}(1) \rangle = \tau(z_j) \times e^{-\bar{N}} \times \left(1 + \sigma_{\mathcal{F}}^2 \left[\frac{\bar{N}^2}{2} - \bar{N} \right] \right) . \quad (11)$$

In general, if there are n lensed sources (at redshifts z_j) in the HDF, then we find

$$\langle \mathcal{L}(n) \rangle = \prod_{j=0}^n \tau(z_j) \times e^{-\bar{N}} \times \left(1 + \sigma_{\mathcal{F}}^2 \left[\frac{\bar{N}^2}{2} - n\bar{N} + \frac{n(n-1)}{2} \right] \right). \quad (12)$$

In order to constrain $\Omega_m - \Omega_\Lambda$, we calculate the likelihood for cases in which the number n of lensed sources present in the HDF is 0, 1, 2, or 3, and for $m_{\text{lim}}=28.5$, 28.0, and 27.5. In order to examine the effect of the luminosity function slope α , we have also calculated the likelihood by varying α by ± 0.1 (the quoted error in SLY) from the best estimate of -2.1 (for source redshifts between 2 and 3).

In Table 2, we present the 95% confidence lower limits on $\Omega_m - \Omega_\Lambda$ for various cases. We define a canonical case in which the lens search has been carried out to $m_{\text{lim}} = 28.5$, and has found one lensed source ($n = 1$) in the HDF with a redshift $z_s = 2.5$. We take $\alpha = -2.1$ in the canonical case. In order to test the effect of different number of lensed sources observed in the HDF, we vary n from this canonical scenario and assume that all lensed sources are at a redshift of 2.5 (this gives the weakest lower limit). The cumulative probabilities for the observed number of lenses, as a function of $\Omega_m - \Omega_\Lambda$, are shown in Figure 3, where the plotted curves represent no lensed sources in HDF (solid), one lensed source (short-dashed), two lensed sources (long-dashed) and three lensed sources (dot-dashed). If there are no lensed sources in the HDF, then at the 95% confidence level $\Omega_m - \Omega_\Lambda > -0.17$, so that in a flat universe $\Omega_\Lambda < 0.58$. If there is one lensed source in the HDF, our constraints depend only slightly on the source redshift. If the source redshift is 1, then $\Omega_m - \Omega_\Lambda > -0.27$, implying $\Omega_\Lambda < 0.63$ in a flat universe. If instead the source redshift is 2.5, then $\Omega_m - \Omega_\Lambda > -0.32$, and hence $\Omega_\Lambda < 0.66$ in a flat universe.

As tabulated in Table 2, the change in I-band lens-search magnitude limit from 28.5 to 27.5 has a surprisingly small effect on the limits on $\Omega_m - \Omega_\Lambda$; the effect of the nondetection of secondary images beyond the limiting magnitude is compensated to some extent by the effect of magnification bias. Except in the case where 3 strongly lensed sources are present in the HDF, $\Omega_m - \Omega_\Lambda > -0.48$ at the 95% confidence level. This implies that in a flat universe $\Omega_\Lambda < 0.74$, which is consistent with the recent cosmological parameter constraints based on the high redshift type Ia supernovae (Riess et al. 1998), and with previous limits on the cosmological constant based on gravitational lensing (see, e.g., Falco et al. 1998; Kochanek 1996; Chiba & Yoshi 1997).

4. SYSTEMATIC ERRORS

4.1. Errors Affecting the Predicted Rate of Lensing

Errors in the photometric redshifts and in F —Our lensing rate calculations rely on the accuracy of photometric redshifts, and hence errors in these redshifts produce errors in the estimated lensing rate. The dispersion of redshifts in, e.g., the WBT catalog with respect to spectroscopically

measured ones, range from 0.03 to 0.1 for $z \lesssim 2$ and 0.14 to 0.36 for $z \gtrsim 2$. The largest effect this would have on the predicted lensing rates would be if the redshifts were *all* systematically low or high, by an amount equal to the quoted error. Even in such an extreme case, the 95% confidence lower limit on $\Omega_m - \Omega_\Lambda$ in our canonical case would only range from -0.39 to -0.23, using respectively redshifts that are all 1σ low and 1σ high compared to the best estimates in the WBT catalog. This is actually a tremendous overestimate of the effect of errors in the photometric redshifts. In reality, a comparison of the photometric redshifts of WBT with available spectroscopic redshifts indicates that the errors are evenly distributed between high and low estimates, so the overall predicted lensing rate is barely affected. The only systematic effect visible in the WBT catalog is a paucity of galaxies in the redshift interval of 1.5 to 2.2. This has a small but visible effect on our $\Omega_m - \Omega_\Lambda$ limits; the results for the WBT catalog are larger than those of the SLY catalog by 2% to 4%. This increase is primarily due to the peaked distribution of galaxies between redshifts of 2 and 2.5 in the WBT catalog, while the same galaxies have a much broader distribution in the SLY catalog. In addition, about 10 galaxies in the WBT catalog with $z \sim 2.5$ have $z < 1$ in the SLY catalog. Nonetheless, the two catalogs yield expected lensing rates that are almost indistinguishable from each other.

Another possible systematic error has to do with the way that the F parameter (eq. [5]) is estimated. One method is to use extensive local surveys of the galaxy luminosity function and velocity dispersions to calculate F , then assume that because most foreground lenses are at a redshift less than unity and galaxy evolution out to that redshift is not believed to be dramatic enough to change F significantly (see Mao & Kochanek 1994), the value of F to use in lensing calculations is the same as it is locally. This is the approach we adopt, and it is supported by the luminosity function in the HDF itself (see § 2.2). Note, however, that if F were to be inferred solely from observations of a particular field, such as the HDF, then because the inferred number density and luminosity of galaxies depends on the assumed cosmology, so will F . The dependence of the inferred F on cosmology also depends on the relation between luminosity and velocity dispersion, but if $\gamma = 4$, the effect is that F is smaller when $\Omega_\Lambda > 0$ than when $\Omega_m = 1$ and $\Omega_\Lambda = 0$, as is often assumed. If $\Omega_m - \Omega_\Lambda \sim -0.4$, the effect is to decrease F by $\sim 30\%$ for lenses between $z = 0.5$ and $z = 1$. If the field of interest contains a small enough number of potential lenses so that fluctuations are important and F must be derived from that field, this effect may have to be included. In the case of the HDF, however, the number counts are large and the expected level of fluctuations is small, so we assume that F is the same as it is locally.

Errors in the lensing rate calculation—Another source of systematic error in our study is that we have used the analytical filled-beam expression to estimate the lensing rate at high redshift. This calculation underestimates the true lensing rate based on numerical techniques by about 2% for the source redshifts of the HDF (Holz et al. 1998). Thus, we have underestimated the true lensing rate in HDF. This is a systematic error in our calculation, and it implies that our lower limits on $\Omega_m - \Omega_\Lambda$ have been underestimated by a similar amount.

We have also assumed that lensing galaxies can be described by isothermal spheres. However,

it is likely that galaxies have a non-negligible core radius. Such a core radius can affect the lensing rate by decreasing the expected number of lensed sources present in the HDF compared to the number calculated assuming a zero core radius. Kochanek (1996) addressed the issue of a finite core radius by studying lens models described by softened isothermal spheres, and showed that a finite core radius increases the velocity dispersion; thus, the decrease in lensing probability due to an added core radius is compensated by the increase in velocity dispersion. In addition, the observed core radii of E and S0 galaxies that dominate the lensing rate are much smaller than their Einstein radii, and hence the effect of a finite core radius is small (Kochanek 1996). We therefore do not expect the effect of finite galaxy core radii to dramatically change the lower limits on $\Omega_m - \Omega_\Lambda$ presented in this paper.

4.2. Errors Affecting the Observed Rate of Lensing

Reddening effects—The extinction of images may be of considerable importance in lens studies. By comparing radio-selected and optical-selected lens samples, Malhotra et al. (1997) suggested that optical lens searches are heavily impaired by extinction due to dust, with a mean magnitude change of 2 ± 1 magnitudes between images. In a magnitude-limited lens search program such as in the HDF, reddening due to dust is expected to decrease the observed number of lensed images, because some may have been reddened beyond the magnitude limit. The effect of reddening due to dust was recently discussed in Falco et al. (1998), who suggest that extinction from dust only produces a mean magnitude change of ~ 0.5 . If this in fact applies to HDF galaxies, then we do not expect any of the lensed sources to redden beyond the magnitude limit of HDF. Kochanek (1996) presented a reddening model in lensing statistics and concluded only a 10% change in lensing probability is due to extinction in galaxies based on observational constraints. Given that there is no detailed analysis of dust distribution associated with HDF galaxies, we do not include the effects of reddening due to dust in the present calculation.

Source confusion and image separation effects—The clustering of optical galaxies may confuse lens search programs in two ways: On the one hand, clustering can lead one to infer the existence of multiply-lensed sources under the assumption that observed sources are images of a lensed background object, when in fact the images are unrelated; while, on the other hand, clustering of galaxies can confuse lensed-image identification by increasing the surface brightness of the surrounding regions near the images. The two gravitationally lensed sources found by Ratnatunga et al. (1995) using HST WFPC images have image separations of the order $\sim 1.2''$ to $1.5''$. For presently confirmed lenses, the effective diameter of the foreground lensing galaxies at $z \sim 1$ are of the order $\sim 1.5''$, similar to lensed image separations. Thus, source clustering may impair the detection of lensed sources. This effect may in fact be present in the currently confirmed lensed source sample, where almost all of the lensed sources with small image separations were initially selected in radio searches. However, gravitationally lensed sources typically have image shapes that can be differentiated from random clustering of galaxies, and generally have colors different

from foreground galaxies. Therefore, a careful examination of the HDF, including both colors and positions, should efficiently reveal lensed sources. The recent discovery of about 10 new small separation lensed sources in the HST Medium Deep Survey (K. Ratnatunga, private communication) suggests that efficient lens searches have been made. Therefore, we do not expect that a large number of HDF lenses have been missed, due to galaxy clustering or source confusion.

5. SUMMARY AND CONCLUSIONS

By comparing the expected number of lensed sources in the HDF to the observed number of lensed sources, we have presented limits on the cosmological parameters. We have considered the possibility that present lens search programs may have missed one to three possible lensed sources in the HDF, and have given our cosmological parameter constraints for a variety of cases, including the change in limiting magnitude for lens searches.

We find that the expected number of lenses in the HDF is primarily a function of $\Omega_m - \Omega_\Lambda$. A comparison of the predicted number of lensed sources with the observed number allows us to put a lower limit on the current value of $\Omega_m - \Omega_\Lambda$. Making use of the HDF luminosity function (as determined by SLY), our 95% confidence lower limit on $\Omega_m - \Omega_\Lambda$ ranges between -0.17 and -0.59 (see Table 2). If the only lensed source in the HDF is the one candidate found by Zepf et al. (1997), then $\Omega_m - \Omega_\Lambda > -0.39$. These lower limits are not in conflict with estimates based on high redshift supernovae (viz., $\Omega_m - \Omega_\Lambda \sim -0.5 \pm 0.4$ [Riess et al. 1998]).

As has been recently noted in the literature, combining $\Omega_m - \Omega_\Lambda$ results from high redshift supernovae measurements with $\Omega_m + \Omega_\Lambda$ results from CMB power spectrum analysis constrains Ω_m and Ω_Λ separately, with much higher accuracy than the individual experiments alone (White 1998; Tegmark et al. 1998). We note that gravitational lensing constraints on $\Omega_m - \Omega_\Lambda$ should also be considered in such an analysis.

We have shown, by comparing our results from two different catalogs, that photometric redshifts can be used to estimate the expected lensing rate with reasonable accuracy. This bodes well for the upcoming Southern Hubble Deep Field redshift catalog that is expected in the near-future. The Southern HDF will double the number of high redshift galaxies and will thus double the expected number of gravitationally lensed sources. If, for example, $\Omega_m - \Omega_\Lambda \sim -0.5$, then from Table 1 there could be as many as a dozen lensed sources detected in the Southern HDF. The actual number of detected sources will lead to strong constraints on $\Omega_m - \Omega_\Lambda$.

We thank Yun Wang, Neta Bahcall, Ed Turner and Marcin Sawicki for making their photometric redshift catalogs publicly available, and Stephen Zepf for useful discussions regarding the observed gravitational lensing rate in the HDF. This work was supported in part by NASA grant NAG 5-2868 (MCM), and by NASA grant NAG 5-4406 and NSF grant DMS 97-09696 (JMQ). ARC acknowledges partial support from the McCormick Fellowship at the University of Chicago,

and a Grant-In-Aid of Research from the National Academy of Sciences, awarded through Sigma Xi, the Scientific Research Society.

REFERENCES

- Bahcall, J. N., et al. 1992, ApJ, 387, 56.
- Chiba, M. & Yoshi, Y. 1997, ApJ, 489, 485.
- Falco, E. E., Kochanek, C. S., Munoz, J. A. 1998, ApJ, 494, 47.
- Fukugita, M., Futamase, T., Kasai, M., Turner, E. L. 1992, ApJ, 393, 3.
- Geller, M. J. et al. 1997, AJ, 114, 2205.
- Gwyn, S. D. J. & Hartwick, F. D. A. 1996, ApJ, 468, L77.
- Hogg, D W. et al. 1996, ApJ, 467, L73.
- Holz, D. E., Miller, M. C., Quashnock, J. M. 1998, ApJ, submitted (astro-ph/9804271).
- Kochanek, C. S. 1991, ApJ, 379, 517.
- Kochanek, C. S. 1993, MNRAS, 261, 453.
- Kochanek, C. S. 1996, ApJ, 466, 638.
- Madau, P. et al. 1996, MNRAS, 283, 1388.
- Madau, P., Pozzetti, L., & Dickinson, M. 1998, ApJ, 498, 106.
- Malhotra, S., Rhoads, J. E., Turner, E. L. 1997, MNRAS, 288, 138.
- Mao, S. D., & Kochanek, C. S., 1994, MNRAS, 268, 569.
- Maoz, D. et al. 1992, ApJ, 394, 51.
- Maoz, D., & Rix, H.-W. 1993, ApJ, 416, 425.
- Ratnatunga, K. U., Ostrander, E. J., Griffiths, R. E., Im, M. 1995, ApJ, 453, L5.
- Riess, A. G. et al. 1998, AJ, in print (astro-ph/9805201).
- Sawicki, M. J., Lin, H., Yee, H. K. C. 1997, AJ, 113, 1. [SLY]
- Tegmark, M., et al. 1998, astro-ph/9805117.
- Wang, Y., Bahcall, N., Turner, E. L. 1998, astro-ph/9804195. [WBT]

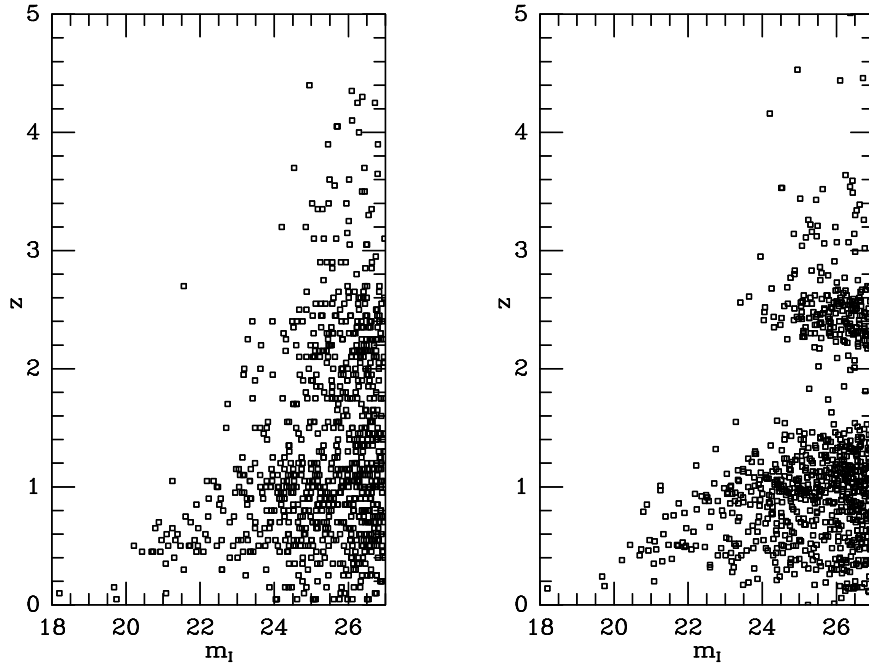


Fig. 1.— Redshift distribution of 848 galaxies with I-band magnitude $\lesssim 27$ in the HDF. The plot shows the photometric redshifts derived by Sawicki, Lee, & Yin (1997; SLY) (*left panel*) and Wang, Bahcall, & Turner (1998; WBT) (*right panel*), as a function of the I-band magnitude. Both catalogs appear to trace the same redshift distribution, with two peaks ($z \sim 0.6$ and 2.3). However, there is a lack of galaxies in the WBT catalog between $z \sim 1.5$ to 2.2 . This is the same range in redshift where no spectroscopic redshifts are currently available for the HDF.

White, M. 1998, astro-ph/9802295.

Williams, R. E. et al. 1996, *AJ*, 112, 1335.

Zepf, S. E. et al. 1997, *ApJ*, 474, L1.

Table 1. Expected Number of Lenses in the HDF.

$\Omega_m - \Omega_\Lambda$	Sawicki, Lee, & Yin 1997	Wang, Bahcall, & Turner 1998
-1.0	28.7	31.7
-0.9	16.5	17.9
-0.8	10.8	11.6
-0.7	8.6	9.2
-0.6	7.0	7.4
-0.5	5.9	6.3
-0.4	5.2	5.5
-0.3	4.6	4.8
-0.2	4.1	4.3
-0.1	3.7	3.9
0.0	3.4	3.6
0.1	3.1	3.3
0.2	2.9	3.0
0.3	2.7	2.8
0.4	2.5	2.6
0.5	2.3	2.4
0.6	2.2	2.3
0.7	2.1	2.1
0.8	2.0	2.0
0.9	1.9	1.9
1.0	1.8	1.9

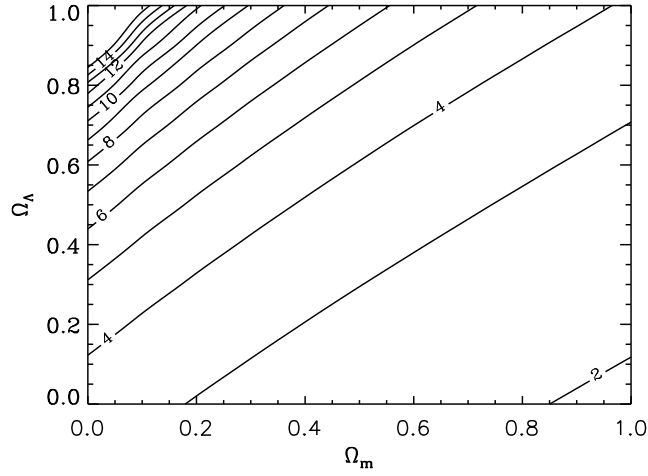


Fig. 2.— Expected number of gravitational lenses, \bar{N} , in the HDF, as a function of Ω_m and Ω_Λ . \bar{N} is constant along lines of constant $\Omega_m - \Omega_\Lambda$, allowing for direct constraints on this quantity. Shown here is the expected number of lenses based on the SLY catalog, and for lens search programs that have been carried out to a limiting magnitude of 28.5 in HDF I-band images.

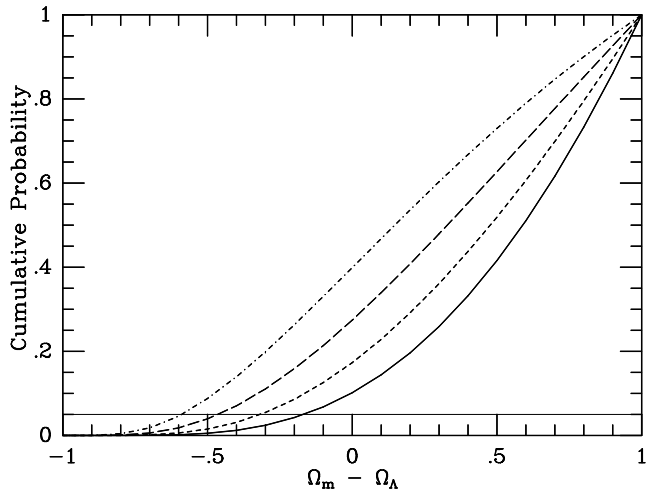


Fig. 3.— Cumulative probability distribution for $\Omega_m - \Omega_\Lambda$, if there is no lensed source (*solid*), one lensed source (*short-dashed*), two lensed sources (*long-dashed*) and three lensed sources (*dot-dashed*) in the HDF, down to a lens-search limiting magnitude of 28.5 in I-band images (using photometric redshifts from the SLY catalog). The intercepts with the horizontal line show the 95% confidence lower limits on $\Omega_m - \Omega_\Lambda$ (see Table 2).

Table 2. 95% confidence lower limits on $\Omega_m - \Omega_\Lambda$.

	Sawicki, Lee, & Yin 1997	Wang, Bahcall, & Turner 1998
$m_{\text{lim}} = 28.5, \alpha = -2.1, n = 1 (z_s = 2.5)$	-0.32	-0.29
$m_{\text{lim}} = 28.5, \alpha = -2.1, n = 0$	-0.17	-0.15
$m_{\text{lim}} = 28.5, \alpha = -2.1, n = 1 (z_s = 1.0)$	-0.27	-0.25
$m_{\text{lim}} = 28.5, \alpha = -2.1, n = 2 (z_s = 2.5)$	-0.47	-0.43
$m_{\text{lim}} = 28.5, \alpha = -2.1, n = 3 (z_s = 2.5)$	-0.59	-0.56
$m_{\text{lim}} = 28.5, \alpha = -2.0, n = 1 (z_s = 2.5)$	-0.39	-0.38
$m_{\text{lim}} = 28.5, \alpha = -2.2, n = 1 (z_s = 2.5)$	-0.30	-0.27
$m_{\text{lim}} = 28.0, \alpha = -2.1, n = 1 (z_s = 2.5)$	-0.39	-0.36
$m_{\text{lim}} = 27.5, \alpha = -2.1, n = 1 (z_s = 2.5)$	-0.48	-0.45